Belief Propagation Receivers for Near-Optimal Detection of Nonlinearly Distorted OFDM Signals

Sergey V. Zhidkov
Cifrasoft Ltd.
Izhevsk, Russia
E-mail: sergey.zhidkov@cifrasoft.com

Rui Dinis
Instituto de Telecomunicações and
Departamento de Engenharia Electrotecnica
Faculdade de Ciłncias e Tecnologia,
Universidade Nova de Lisboa, Almada, Portugal
E-mail: rdinis@fct.unl.pt

***Abstract*—It is generally assumed that nonlinear distortion effects in multicarrier systems can lead to substantial performance degradation. However, it was recently shown that the nonlinear distortion component contains information on the transmitted signal and can be used to improve the performance. Nonetheless, all known receivers that are able to take advantage of this fact are extremely complex. In this paper, we present receivers based on the generalized approximate message passing concept for orthogonal transform multiplexing (OFDM) signals with strong nonlinear effects. Our simulation results show that the proposed receivers are very powerful, allowing excellent performance in the presence of strong nonlinear distortions. In fact, nonlinear OFDM schemes using those receivers can outperform linear OFDM schemes by several dBs in ideal additive white Gaussian noise (AWGN) channels, and by tens of dBs in frequency-selective fading channels.**

***Index Terms*—OFDM, nonlinearity, belief propagation, approximate message passing.**

I. Introduction

The most popular transmission technique for broadband communication over time-dispersive channels is orthogonal frequency division multiplexing (OFDM). This is due to its robustness to severe time-dispersive effects without the need of complex receiver implementations. For this reason, OFDM and other multicarrier modulation schemes were selected for digital terrestrial broadcasting and are the main modulations for 4G systems (also known as LTE (Long Term Evolution)). OFDM schemes and other multicarrier variations are also expected to be the main transmission techniques for 5G systems.

However, multicarrier signals in general, and OFDM signals in particular, are very prone to nonlinear distortion effects, namely those associated with power amplifiers [1]. By employing the Bussgang theorem [2], the nonlinearly distorted signal can be decomposed as the sum of an useful component, proportional to the original signal, and an uncorrelated nonlinear distortion component. Since the nonlinear distortion term is approximately Gaussian at the subcarrier level [3], it behaves as an additional Gaussian, noise-like term. Therefore, the general assumption is that it can lead to substantial performance degradation with high irreducible error floors [4]. By employing the so-called Bussgang receivers [5], one tries to estimate and cancel the nonlinear distortion term. The problem with this type of receivers is that the estimation of the nonlinear distortion is difficult, especially at low SNR (Signal-to-Noise Ratio) due to error propagation effect. And, even if we could achieve perfect cancellation of the nonlinear distortion term, there would still be some performance degradation relatively to the linear case due to the power ”wasted” in the nonlinear distortion component.

However, the non-linear distortion term is a function of the original OFDM signal and, therefore, contains information about it. In fact, it was recently shown that the optimum performance of nonlinear OFDM can even be better than the linear one [6], [7]. However, this means employing optimum receivers, whose complexity grows exponentially with the block length, making them too complex, even for small number of OFDM subcarriers. Although, several sub-optimum receivers were proposed for nonlinear OFDM [6], [8], their performance falls far from the the optimum performance and/or their complexity is still extremely high.

A promising class of receivers for nonlinear OFDM was proposed in [10]. These receivers are based on the general approximate message passing algorithm [11]–[14], but are only suitable for nonlinearities operating on real-valued multicarrier signals. However, the most common nonlinear operations on OFDM signals are modelled as bandpass memoryless nonlinearities (also called polar nonlinearities) [3]. They include most common power amplifiers (e.g., traveling wave tube amplifiers (TWTA) [15] and solid state power amplifiers (SSPA) [16]), as well as envelope clipping operations, widely employed to reduce the peak-to-average power ratio (PAPR) [17].

In this paper, we consider OFDM schemes with strong nonlinear distortion effects associated with bandpass memoryless nonlinearities and present powerful receivers able to approach the optimal performance. Our receivers can be regarded as an extension for the continuous-time bandpass memoryless nonlinearities of the ones proposed in [10] for real-valued and Nyquist-rate sampled nonlinearities.

This paper is organized as follows. In Section II, we present the OFDM system model with polar nonlinearity. In Section III, message passing receivers for nonlinearly distorted OFDM signals are proposed and their performance is studied by means of computer simulation in Section IV. Finally, Section V draws conclusions.

II. System Model

A. Transmitter and channel model

In this paper, we consider a point-to-point multicarrier communication system depicted in Figure 1. In each symbol interval, a block of $N\log_2(M)$ bits is first mapped into an N-point vector $\mathbf{x}^{(data)} = [x_0\, x_1 \ldots x_{N-1}]^T$ using M-ary quadrature amplitude modulation (M-QAM). The M-QAM modulated vector is then transformed into NJ-vector $\mathbf{x}$ by adding $N(J-1)/2$ zeros at the edges of the block, where J is the oversampling factor. The frequency-domain vector $\mathbf{x}$ is transformed into the time domain via inverse discrete Fourier transform (IDFT) operation:

$$\mathbf{z} = \mathbf{F}\mathbf{x}, \tag{1}$$

where $\mathbf{F}$ is NJ by NJ matrix with elements

$$F_{n,k} = \frac{1}{\sqrt{NJ}} e^{-\frac{j2\pi nk}{NJ}}, \quad n,k = 0,...,NJ-1, \tag{2}$$

A cyclic prefix (CP) of length $N_{cp}J$ is appended to the time-domain vector $\mathbf{z} = [z_0\, z_1 \ldots z_{NJ-1}]^T$, and then the sequence $\{z_n\}$ is passed through a memoryless nonlinear block $f(z)$, leading to the samples

$$y_n = f(z_n), \quad n = -N_{cp}J,...,NJ-1 \tag{3}$$

Nonlinear distortions introduced in $f(z)$ may lead to strong out-of-band (OOB) radiation due to spectral regrowth effects. Optionally, the OOB emission can be partially or totally suppressed by the OOB-filtering (OOBF) block.

After that the signal $\{y_n\}$ is transmitted via multipath channel with impulse response $\{h_n\}$ and the received signal can be finally represented as

$$r_n = y_n * h_n + w_n \tag{4}$$

where '$*$' denotes the cyclic convolution (equivalent to a linear convolution at the useful part of the OFDM block when appropriate cyclic prefixes are employed) and w_n is the additive white Gaussian noise (AWGN) term, with zero mean and variance σ_w^2. Due to the presence of cyclic prefix the received signal can be represented in the frequency domain as:

$$R_k = H_k Y_k + W_k, \tag{5}$$

where $\{R_k\}$, $\{H_k\}$, $\{Y_k\}$, and $\{W_k\}$, $k = 0,1,...,NJ-1$ are the DFTs of the signals $\{r_n\}$, $\{h_n\}$, $\{y_n\}$, and $\{w_n\}$, respectively.

B. Memoryless nonlinearity models

In this paper, we consider bandpass memoryless nonlinearities (also denoted polar nonlinearities) described by AM/AM and AM/PM conversion characteristics. Under this assumption, the memoryless nonlinear function $f(z)$ can be represented by the following decomposition [4]:

$$f(z_n) = f_A(|z_n|)\, e^{j(f_\Theta(|z_n|) + \arg(z_n))}, \tag{6}$$

where $f_A(|z_n|)$ is the AM/AM conversion function, and $f_\Theta(|z_n|)$ is the AM/PM conversion function. Throughout this paper, we consider two types of polar nonlinearities. The first one is a soft envelope limiter (SEL), which can be regarded as a model of ideally pre-distorted amplifier [4]:

$$\begin{aligned} f_A(|z_n|) &= \begin{cases} |z_n|, & |z_n| \le s_M \\ s_M, & |z_n| > s_M \end{cases} \\ f_\Theta(|z_n|) &= 0 \end{aligned} \tag{7}$$

with s_M denoting the envelope clipping threshold. An ideal soft clipping is also the model for the envelope clipping usually employed for reducing the PAPR of OFDM [3], [17]. The second one is the travelling wave tube amplifier (TWTA) model (namely, the Saleh model [15]), where

$$\begin{aligned} f_A(|z_n|) &= \frac{2|z_n|}{s_M\left(1+\left(\frac{|z_n|}{s_M}\right)^2\right)} \\ f_\Theta(|z_n|) &= \frac{2\theta_M |z_n|^2}{s_M^2\left(1+\left(\frac{|z_n|}{s_M}\right)^2\right)} \end{aligned} \tag{8}$$

with s_M denoting the saturation level and θ_M denoting the phase displacement at saturation point. It should be noted that our results are also applicable to other types of polar memoryless nonlinearities.

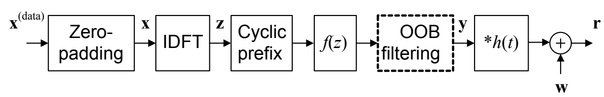

Fig. 1. The transmitter and channel model.

III. Belief Propagation Receiver and Channel Equalizer

A. Generalized approximate message passing algorithm

In case of an ideal AWGN channel and without OOB filtering, the model of the received signal $\mathbf{r} = [r_0\, r_1 \ldots r_{NJ-1}]^T$ can be simplified to

$$\mathbf{r} = f(\mathbf{F}\mathbf{x}) + \mathbf{w}, \tag{9}$$

where $\mathbf{w} = [w_0\, w_1 \ldots w_{NJ-1}]^T$ (as usual, we assume that the cyclic prefix is discarded at the receiver side and it is not used by the decoder). The model (9) is equivalent to a general problem statement for the generalized approximate message passing (GAMP) algorithm [11], which belongs to a class of Gaussian approximations of loopy belief propagation for dense graphs. The sum-product variant of the GAMP algorithm approximates the minimum mean-squared error (MMSE) estimates of $\mathbf{z}$ and $\mathbf{x}$. The canonical GAMP algorithm with damping [12], [13] is summarized in Algorithm 1.

Each iteration of the GAMP algorithm consists of four basic steps: (a) output linear step, (b) output non-linear step, (c) input linear step, and (d) input non-linear step. The output linear step produces estimates of intermediate vector $\{\hat{p}_n\}$, $n = 0,1,...,NJ-1$ with corresponding variances $\{\mu_n^p\}$. The output non-linear step produces estimates of intermediate vector $\{\hat{s}_n\}$ with corresponding variances $\{\mu_n^s\}$. Likewise, the input linear step produces estimates of intermediate vector $\{\hat{v}_n\}$ with corresponding variances $\{\mu_n^v\}$, and finally, the input

Algorithm 1 GAMP decoder algorithm (with damping)

Input: $\mathbf{r}$
Output: $\hat{\mathbf{x}}$
Parameters: t_{max}, $\mathbf{F}$, $g_{in}(\cdot)$, $g_{out}(\cdot)$, σ_w^2, β

1) Initialization:
$t=1,\ \hat{\mathbf{x}}(1)=\mathbf{0}_{NJ,1},\ \hat{\mathbf{s}}(0)=\mathbf{0}_{NJ,1},\ \mu^x(1)=\mathbf{1}_{NJ,1}$

2) Output linear step:
$\mu_n^p(t)=\frac{1}{NJ}\sum\limits_{k=0}^{NJ-1}\mu_k^x(t),\forall n$
$\hat{p}_n(t)=\sum\limits_{k=0}^{NJ-1}F_{n,k}\hat{x}_k(t)-\mu_n^p(t)\,\hat{s}_n(t-1),\forall n$

3) Output non-linear step:
$\hat{s}_n(t)=(1-\beta)\hat{s}_n(t-1)+\beta g_{out}(\hat{p}_n(t),\mu_n^p(t),r_n),\forall n$
$\mu_n^s(t)=(1-\beta)\mu_n^s(t-1)-\beta\frac{\partial}{\partial\hat{p}}g_{out}(\hat{p}_n(t),\mu_n^p(t),r_n),\forall n$

4) Input linear step:
$\tilde{x}_k(t)=(1-\beta)\,\tilde{x}_k(t-1)+\beta\hat{x}_k(t),\forall k$
$\mu_k^v(t)=\left(\frac{1}{NJ}\sum\limits_{n=0}^{NJ-1}\mu_n^s(t)\right)^{-1},\forall k$
$\hat{v}_k(t)=\tilde{x}_k(t)+\mu_k^v(t)\sum\limits_{n=0}^{NJ-1}F_{n,k}^{*}\hat{s}_k(t),\forall k$

5) Input non-linear step:
$\hat{x}_k(t+1)=g_{in}(\hat{v}_k(t),\mu_k^v(t)),\forall k$
$\mu_k^x(t+1)=-\mu_k^v(t)\frac{\partial}{\partial\hat{v}}g_{in}(\hat{v}_k(t),\mu_k^v(t)),\forall k$

Increment $t\to t+1$ and return to step 2) until t_{max} iterations have been performed.

non-linear step produces estimates of the $\{\hat{x}_n\}$ and $\{\mu_n^x\}$, respectively. Since $\mathbf{F}$ is the Fourier transform matrix, the input and output linear steps of the GAMP algorithm can be efficiently implemented using fast Fourier transform operations. Scalar nonlinear functions $g_{in}(\cdot)$, ${g'}_{in}(\cdot)$, and $g_{out}(\cdot)$, ${g'}_{out}(\cdot)$, depend on the employed modulation format and the shape of non-linearity $f(z)$, and will be discussed in more detail in the next subsection. A general hardware architecture of the GAMP decoder (without dumping, that is when $\beta=1$) is illustrated in Figure 2.

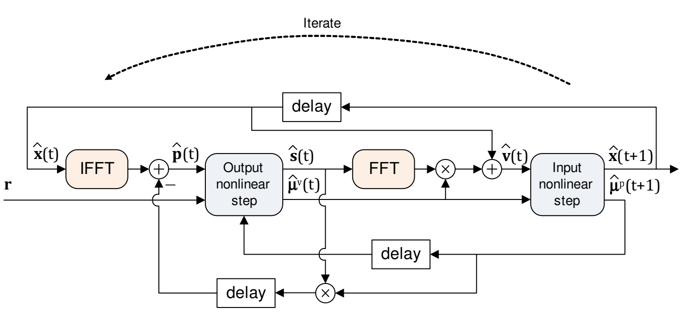

Fig. 2. GAMP decoder architecture.

B. Input non-linear step

To implement sum-product loopy belief propagation algorithm the input non-linear functions $g_{in}(\cdot)$, ${g'}_{in}(\cdot)$ should be selected as [11]

$$g_{in}(\hat{v},\mu^v):=\mathrm{E}\left[x|\,\hat{v}\right] \tag{10}$$

and

$$\mu^v\frac{\partial}{\partial\hat{v}}g_{in}(\hat{v},\mu^v):=\mathrm{var}\left[x|\,\hat{v}\right] \tag{11}$$

(for clarity, from hereafter we omit the iteration number t and the element index k). This approximation relies on the notion that in the GAMP algorithm v is interpreted as a Gaussian noise corrupted version of x with noise variance equal to μ^v. Therefore, for uncoded M-QAM modulation, the input non-linear step can be expressed as

$$\mathrm{E}\left[x|\,\hat{v}\right]=\sum_{i=1}^{M}d_iP\left(d_i|\hat{v},\mu^v\right) \tag{12}$$

and

$$\mathrm{var}\left[x|\,\hat{v}\right]=\sum_{i=1}^{M}\left(d_i-\mathrm{E}\left[x|\,\hat{v}\right]\right)^2P\left(d_i|\hat{v},\mu^v\right), \tag{13}$$

where $\{d_i\}$, $i=1,2,...,M$ is the set of M-QAM constellation points, e.g. $\mathbf{d}=\frac{1}{\sqrt{2}}\left[\begin{array}{cccc}1+j & 1-j & -1+j & -1-j\end{array}\right]$ for 4-QAM constellation, and conditional probabilities $P\left(d_i|\hat{v},\mu^v\right)$ can be evaluated as

$$P\left(d_i|\hat{v},\mu^v\right)=\frac{\exp\left(-\frac{|d_i-\hat{v}|^2}{2\mu^v}\right)}{\sum\limits_{l=1}^{M}\exp\left(-\frac{|d_l-\hat{v}|^2}{2\mu^v}\right)}. \tag{14}$$

Finally, for out-of-band sub-carriers, $\mathrm{E}\left[x|\,\hat{v}\right]=0$ and $\mathrm{var}\left[x|\,\hat{v}\right]=0$.

C. Output non-linear step

By following the approach of [11], the output function $g_{out}(\hat{p},\mu^p,r)$ to implement approximate belief propagation for the MMSE estimation is given by

$$g_{out}(\hat{p},\mu^p,r):=\frac{\hat{z}_0-\hat{p}}{\mu^p},\quad \hat{z}_0:=E\left[z|\,\hat{p},r,\mu^p\right] \tag{15}$$

where the expectation is taken over distribution $p\left(z|\,\hat{p},r,\mu^p\right)$:

$$p\left(z|\,\hat{p},r,\mu^p\right)\propto\exp\left(-\frac{\left\|r-f\left(z\right)\right\|^2}{2\sigma_w^2}-\frac{\left\|\hat{p}-z\right\|^2}{2\mu^p}\right). \tag{16}$$

Likewise, the negative derivative of $g_{out}(\cdot)$ is given by [11]

$$-\frac{\partial}{\partial\hat{p}}g_{out}\left(\hat{p},r,\mu^p\right)=\frac{1}{\mu^p}\left(1-\frac{\mathrm{var}\left[z|\,\hat{p},r,\mu^p\right]}{\mu^p}\right). \tag{17}$$

For the general non-linear model (6), the expectation $E\left[z|\,\hat{p},r,\mu^p\right]$, and variance $\mathrm{var}\left[z|\,\hat{p},r,\mu^p\right]$ can be expressed as

$$\begin{aligned}E\left[z|\,\hat{p},r,\mu^p\right]&=I_1/I_0,\\ \mathrm{var}\left[z|\,\hat{p},r,\mu^p\right]&=I_2/I_0-\left(I_1/I_0\right)^2,\end{aligned} \tag{18}$$

where integrals I_q, $q=0,1,2$ are given in (18) at the top of the next page, and $A_p=|p|$, $A_r=|r|$, $\theta_p=\arg(p)$,

$$I_q = \int_0^\infty \int_0^{2\pi} A_z^{q+1} e^{j\theta_z (q \bmod 2)} e^{-\frac{A_r^2 + f_A^2(A_z) - 2A_r f_A(A_z)\cos\left(\theta_r - \theta_z - f_\theta(A_z)\right)}{2\sigma_w^2} - \frac{A_p^2 + A_z^2 - 2A_p A_z \cos\left(\theta_p - \theta_z\right)}{2\mu^p}} d\theta_z dA_z \tag{18}$$

$\theta_r = \arg(r)$. Unfortunately, for the general nonlinearity model (6), the integrals of (18) cannot be expressed in closed-form using elementary functions. Therefore, in this paper, we obtained (18) using numerical integration. Although the output non-linear step appears complicated, in essence, it is a scalar operation that takes as an input two complex variables $\hat{p}$ and r, two real parameters σ_w and μ^p, and outputs a single complex value $g_{out}(\hat{p}, \mu^p, r)$ and a real value $-\frac{\partial}{\partial \hat{p}} g_{out}(\hat{p}, r, \mu^p)$.

D. Equalization for frequency-selective channels

Canonical approximate message passing algorithms, including GAMP (Algorithm 1), assume that the underlying random variables are independent. In frequency-selective channels, however, this assumption does not hold, since the channel introduces statistical dependencies between the elements of received vector $\{r_n\}$. One way to solve this issue is to use hybrid-GAMP algorithm that combines approximate message passing and standard loopy belief propagation techniques [14]. However, the hybrid-GAMP algorithm may quickly become impractical for complex multipath channels with long impulse response $\mathbf{h}$. On the other hand, it will be shown that the canonical GAMP algorithm combined with a simple minimum-mean-squared error (MMSE) frequency-domain equalizer (FDE) [18] may achieve reliable operation over typical frequency-selective fading channels.

In the FDE equalizer the received vector $\mathbf{r}$ is first transformed into the frequency domain vector $\mathbf{R} = [R_0 R_1 ... R_{NJ-1}]$ by means of DFT, i.e. $\mathbf{R} = \mathrm{DFT}(\mathbf{r})$. The frequency-domain equalized signal $\{R_n^{(eq)}\}$ is given by

$$R_n^{(eq)} = R_n \frac{H_n^*}{|H_n|^2 + \sigma_w^2}, \quad n = 0, 1, ..., NJ-1 \tag{19}$$

where $\{H_n\}$ is the DFT of channel impulse response $\mathbf{h}$ zero-padded to length NJ. The output of equalizer $\mathbf{r}^{(eq)} = \mathrm{IDFT}\left(\mathbf{R}^{(eq)}\right)$, is then used as an input to the conventional GAMP algorithm (Algorithm 1). A similar approach is often used in single-carrier systems with cyclic prefix, also denoted SC-FDE (Single-Carrier with Frequency-Domain Equalization) [18] or in constant envelope OFDM systems [19].

E. Out-of-band emission filtering

As pointed out, when an OFDM signal is submitted to a nonlinear device we have not only in-band distortion, but also OOB radiation due to the spectral widening effects associated with the nonlinear operation. Since the out-of-band radiation has information on the OFDM signal, it is an useful part of the transmitted signal when we consider optimum detection or sub-optimum receivers that try to approach the optimum performance, as the GAMP receiver that we are considering in this paper, and should be taken into account by the receiver.

On the other hand, the spectral widening is undesirable in most OFDM-based systems, since it makes difficult to fulfill required spectral masks, especially for the strongly nonlinear characteristics that we are considering. For this reason it is preferable to have some filtering operation after the nonlinear operation. The total removal of OOB radiation is simple if the nonlinear operation is done in the digital-domain (as with clipping and filtering techniques), although some residual out-of-band signal is unavoidable when the nonlinear operation is associated with power amplification, since it is difficult to perform a highly selective filtering at the output of the power amplifier.

Although the "post-nonlinearity filtering" is not different from the filtering operation associated with the frequency-selective fading channel, a frequency-domain MMSE equalizer is not able to recover the out-of-band signal. However, as we will show in the following, since the fraction of power associated with the OOB signal is relatively small, the performance of our GAMP receivers is still very good when we resort to OOB filtering.

IV. Performance Results

In this section, we provide BER performance results for the decoding and equalization algorithms proposed in this paper for quasi-optimum detection of nonlinear OFDM schemes. Unless stated otherwise, we consider an OFDM system with $N = 1024$ subcarriers, each one with 4-QAM modulation and Grey mapping. The oversampling factor is $J = 4$ and we consider two nonlinearity models, the ones of (7) and (8), which are assumed to be known by the receiver. The integration required by (18) was performed numerically using the midpoint rule. Whenever employed, the out-of-band filtering is ideal, i.e., it removes all out-of-band radiation (the use of more realistic filtering schemes leads only to minor changes in our performance results). We also assumed perfect synchronization and channel estimation at the receiver. The maximum number of iterations of the GAMP algorithm was set to $t_{max} = 25$. The first 12 iterations were performed with damping parameter $\beta = 0.875$, and the remaining with $\beta = 1$. A cyclic-redundancy check (CRC) was appended to each data block, allowing an early stopping criterion, as explained in [9].

A. Optimal Input Saturation Level

Our first goal is to find out the optimal input saturation level s_M/σ, where σ^2 is the variance of $\{z_n\}$, for nonlinearities (7) and (8). As was previously demonstrated in [7], if the optimal decoder is used at the receiver side, the BER performance of nonlinearly distorted OFDM can be better than that of linear OFDM, with larger gains for strongly nonlinear characteristics (i.e., low values of s_M/σ). However, for very small ($s_M/\sigma \rightarrow$

0) the BER performance is limited by the capacity of an ideal hard limiter [20]. Therefore, it is reasonable to assume that there is an optimal saturation level ($0 \leq s_M/\sigma < \infty$), below which the BER performance starts to degrade or, at least, does not improve. Figure (3) shows the BER results vs input saturation level, obtained by simulation for two nonlinearities (SEL and TWTA) at a fixed signal-to-noise ratio per bit ($E_b/N_0 = 2dB$ and $E_b/N_0 = 3.75dB$ for TWTA and SEL nonlinearity, respectively). Based on these results, we may conclude that the optimal saturation level for TWTA nonlinearity is around $s_M/\sigma \approx 0.5$, and the optimal saturation level for SEL is $s_M/\sigma \approx 0$ (i.e., an ideal hard limiter). It should be noted that these saturation levels correspond to strongly nonlinear regimes. In such a case, the spectral regrowth becomes significant (and may be unacceptable for many practical applications), whereas traditional linear receivers become totally ineffective.

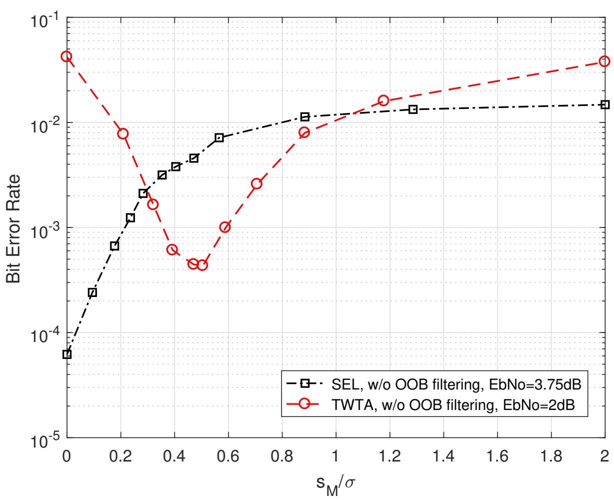

Fig. 3. Impact of the normalized saturation level s_M/σ on the BER performance when $E_b/N_0 = 2dB$ (TWTA) and $E_b/N_0 = 3.75dB$ (SEL)

B. BER Performance in an Ideal AWGN Channel

Figure 4 shows the BER performance of the nonlinear OFDM systems with our GAMP-based receiver. Clearly, the BER performance of nonlinear OFDM system can be significantly better than that of the linear OFDM. For example, the uncoded OFDM system with TWTA nonlinearity (8) with normalized saturation level $s_M/\sigma = 0.5$ and no OOB filtering has an amazing 6.9dB gain over uncoded linear OFDM system at BER=10^{-5}. SEL nonlinearity (7) without OOB filtering also demonstrates significant performance improvement (5.6dB at BER=10^{-5}). With OOB filtering at the transmitter, the BER performance is still better than that of linear OFDM, although, in that case, the performance gain is smaller. This can be explained by two factors: (a) the filtering operation removes a signal that has some information on the transmitted signal and (b) the sub-optimality of the GAMP algorithm, which is designed assuming that there is no OOB filtering. It should also be noted that the TWTA normalized clipping level was not optimized for the case with OOB filtering.

Figure 4 shows the BER performance of a nonlinear OFDM system where the nonlinear operation is done at a sampled version of the OFDM signal at the Nyquist rate, i.e., without oversampling ($J = 1$). In that case, there is no spectral regrowth issue because all nonlinear distortion components fall in-band. Nonetheless, the BER performance is even slightly better than with oversampling and OOB filtering. This is probably due to the fact that in case of Nyquist rate sampling the canonical GAMP algorithm is a closer approximation to the optimal decoder, while in case of OOB filtering it is apparently sub-optimal.

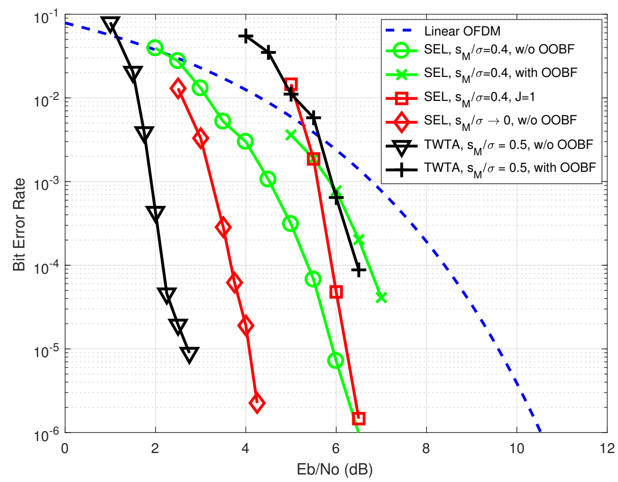

Fig. 4. BER performance for an ideal AWGN channel with the proposed receiver.

C. BER Performance in Frequency Selective Channels

Clearly, OFDM schemes are not usually employed in ideal AWGN channels. Therefore, we considered also the performance of our proposed receiver, which combines GAMP-based decoding and MMSE frequency-domain filtering, when the transmission is made over a frequency-selective multipath channel. We considered a multipath channel with 56 symbol-spaced components, with uncorrealted Rayleigh-distributed fading and exponential power delay profile (PDP) with RMS delay-spread $\tau_{rms} = 14T_s$, where T_s is the sampling interval.

Figure 5 shows BER performance of the OFDM system with SEL nonlinearity in frequency-selective Rayleigh fading channel (with and without OOB filtering). As one can see, in such channel conditions, the nonlinear OFDM with MMSE FDE and GAMP receiver allows a huge gain when compared to linear OFDM. These results are not surprising, since the performance of conventional OFDM schemes in frequency-selective channels is very poor without channel coding, and the nonlinear effects have inherent diversity effects that allow substantial performance gains (see, e.g. [6], [19]).

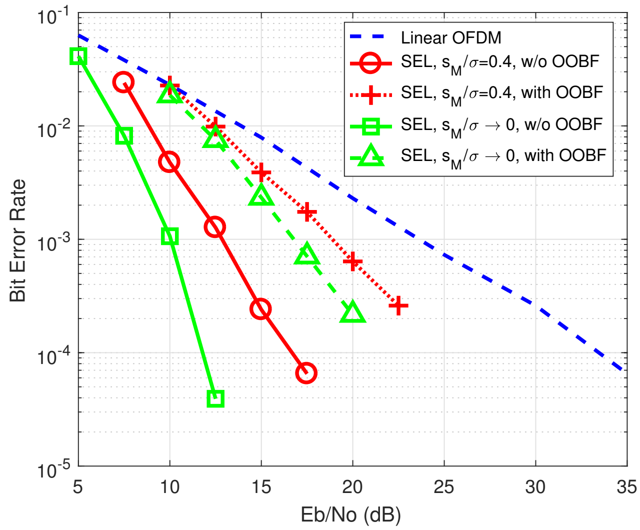

Fig. 5. The proposed receiver BER performance in Rayleigh fading channel

V. Conclusions

In this paper, we proposed a GAMP-based receiver for nonlinearly distorted OFDM signals. We demonstrated that such a receiver can be successfully used when the OFDM signal is affected by bandpass memoryless nonlinearities with different AM/AM and AM/PM conversion functions, with and without OOB filtering. The basic complexity of the approximate message passing receiver for nonlinearly distorted OFDM signals is moderate. It relies on FFT and nonlinear scalar operations, typically requiring only about 10 iterations.

Our simulation results show that in AWGN channel the uncoded nonlinear OFDM may significantly outperform a conventional linear OFDM. What is really remarkable is the fact that significant performance gains can be achieved in AWGN channel for traditional models of non-linear amplifiers (e.g., soft envelope limiter or a TWTA model), which are commonly viewed as "hardware impairments". Furthermore, our GAMP receiver combined with an MMSE-based FDE equalizer demonstrates robust performance in typical frequency-selective fading channels.

References

[1] L. Cimini, "Analysis and simulation of a digital mobile channel using orthogonal frequency division multiplexing," IEEE Trans. Commun., vol. 33, no. 7, pp. 665-675, July 1985

[2] H. Rowe, Memoryless nonlinearities with Gaussian input: elementary results, Bell System Tech. Journal, vol. 61, no. 67, pp. 1519-1526, Sep. 1982

[3] T. Araújo and R. Dinis, Analytical Evaluation of Nonlinear Distortion Effects on Multicarrier Signals, CRC Press, Taylor & Francis Group, 2015

[4] P. Banelli and S. Cacopardi, "Theoretical analysis and performance of OFDM signals in nonlinear AWGN channels," IEEE Trans. Commun., vol. 48, no. 3, pp. 430-441, Mar. 2000

[5] J. Tellado, L. M. C. Hoo and J. M. Cioffi, "Maximum-likelihood detection of nonlinearly distorted multicarrier symbols by iterative decoding," IEEE Trans. Commun., Vol. 51, No. 2, pp. 218-228, Feb. 2003

[6] J. Guerreiro, R. Dinis and P. Montezuma, "Optimum and sub-optimum receivers for OFDM signals with strong nonlinear distortion effects," IEEE Trans. Commun., vol. 61, no. 9, pp. 3830-3840, Sept. 2013

[7] J. Guerreiro, R. Dinis and P. Montezuma, "On the optimum multicarrier performance with memoryless nonlinearities," IEEE Trans. Commun., vol. 63, no. 2, pp. 498-509, Feb. 2015

[8] J. Guerreiro, M. Beko, R. Dinis, P. Montezuma, Using the Fireworks Algorithm for ML Detection of Nonlinear OFDM, IEEE VTC2017 (Fall), Toronto, Canada, Sept. 2017

[9] S. V. Zhidkov, "Orthogonal transform multiplexing with memoryless nonlinearity: a possible alternative to traditional coded-modulation schemes, in Proc. 9th Int. Congress on Ultra Modern Telecommunications and Control Systems (ICUMT-2017), Munich, Germany, Nov., 2017

[10] S. V. Zhidkov, "Detection of nonlinearly distorted OFDM signals via generalized approximate message passing," arXiv:1703.01562 [cs.IT], Mar. 2017

[11] S. Rangan, "Generalized approximate message passing for estimation with random linear mixing," in Proc. IEEE Int. Symp. Information Theory, Saint-Petersburg, Russia, 2011, pp. 2174-2178. (extended version available at arXiv:1010.5141 [cs.IT]).

[12] S. Rangan, P. Schniter, and A. Fletcher, "On the convergence of generalized approximate message passing with arbitrary matrices," in Proc. IEEE Int. Symp. Information Theory, July 2014, pp. 236240, (extended version available at arXiv:1402.3210 [cs.IT]).

[13] J. Vila, P. Schniter, S. Rangan, F. Krzakala and L. Zdeborov, "Adaptive damping and mean removal for the generalized approximate message passing algorithm," in Proc. IEEE Int. Conf. on Acoustics, Speech and Signal Processing (ICASSP), South Brisbane, QLD, 2015, pp. 2021-2025

[14] S. Rangan, A. K. Fletcher, V. K Goyal, E. Byrne, P. Schniter, "Hybrid approximate message passing." IEEE Trans. Signal Processing, Vol. 65, Issue 17, 2017, pp. 4577 - 4592.

[15] A.A.M. Saleh, "Frequency-independent and frequency-dependent nonlinear models of TWT amplifiers," IEEE Trans. Commun., vol. COM-29, pp.1715-1720, Nov. 1981.

[16] C. Rapp, "Effects of HPA-nonlinearity on a 4- DPSK/OFDM-signal for a digital sound broadcasting system," In Proc. 2nd European Conference on Satellite Communications, pages 179184, October 1991.

[17] Y. Rahmatallah and S. Mohan, "Peak-to-average power ratio reduction in OFDM systems: a survey and taxonomy," IEEE Commun. Surveys Tuts., vol. 15, no. 4, pp. 15671592, Mar. 2013.

[18] D. Falconer, S. L. Ariyavisitakul, A. Benyamin-Seeyar and B. Eidson, "Frequency domain equalization for single-carrier broadband wireless systems," IEEE Communications Magazine, vol. 40, no. 4, pp. 58-66, April 2002.

[19] S. C. Thompson, A. U. Ahmed, J. G. Proakis, J. R. Zeidler and M. J. Geile, "Constant envelope OFDM," IEEE Trans. Commun., vol. 56, no. 8, pp. 1300-1312, August 2008.

[20] P. Zillmann, G. R. Fettweis, "On the capacity of multicarrier transmission over nonlinear channels," in Proc. IEEE 61st Vehicular Technology Conference, Vol. 2, pp. 1148-1152, Stockholm, Sweden, May, 2005